Numerical Investigation of the Interaction of Opposing Jets and Supersonic Free Flows



# Numerical Investigation of the Interaction of Opposing Jets and Supersonic Free Flows

ZhiKan Liu<sup>1,2</sup>, YiLun Liu<sup>1,2</sup>, QuanZheng Li<sup>1,2</sup>, Gang Wang<sup>1,2</sup>\*

<sup>1</sup>School of Aeronautics, Northwestern Polytechnical University, Xi'an, 710072, China <sup>2</sup>National Key Laboratory of Aircraft Configuration Design, Xi'an, 710072, China \* Corresponding Author: wanggang@nwpu.edu.cn

#### **Abstract**

Controllable jet emission is commonly used on space vehicles to achieve sustainable favourable attitude. In this paper, a numerical study was presented on the flow physics of a jet emitted from a spherical object opposite to a supersonic freestream at a Mach number (Ma) of 2.5. Three-dimensional simulations are conducted to investigate the intricate counteracting interaction between the jet and the surrounding supersonic flow by solving the Reynolds-Averaged Navier-Stokes equations coupled with the standard Shear Stress Transport (SST) turbulence model. The analysis puts an emphasis on the interaction between shock waves and shear layers at different physical setup, e.g., various total pressure ratios.

The results successfully reproduce two distinguishing interaction modes, i.e., the Long Penetration Mode (LPM) and the Short Penetration Mode (SPM). They are associated with different total pressure ratios. At low total pressure ratios, the LPM and SPM modes emerge alternatively. When the total pressure ratio reached a sufficiently high level, only the SPM occurs. During the Short Penetration Mode, it was observed that the shock stand-off distance, the position of the Mach disc, and the development of the recirculation zone are influenced by the total pressure ratio. In addition, the Long Penetration Mode is shown to be actually an unsteady oscillatory process, which is analyzed using the Dynamic Mode Decomposition (DMD) technique to study the flow motion. The present results suggest that the use of DMD enables the identification of the most unstable modal structures and corresponding temporal frequencies, as well as spatial information, for studying both linear and nonlinear phenomena. Specifically, the dominant pattern found in the cross-sectional plane has an axisymmetric nature, offering essential understanding of the physics involved in the interaction between a jet and supersonic flow moving in opposite directions.

Keywords: Opposing jet; Dynamic mode decomposition; Long penetration mode; Short penetration mode

#### 1. Introduction

The occurrence of the counterflowing jet in supersonic flows has attracted considerable attention in recent decades due to its many applicability and the complex nature of its underlying physics. Several research studies[1-2] have investigated the utilization of a forward-facing cavity, opposing jets, and an aerospike in various configurations. Experiments[3-5] undertaken over time have consistently shown that using an opposing flow from the front body area can significantly reduce both heat and drag experienced by blunt body. These experiments involved testing different combinations of shapes and conditions. In previous research[6-7], it was shown that by injecting a gas in a direction opposed to the flow of air, a technique known as counter flowing may be used to manipulate the shock wave. This manipulation results in a reduction in the surface pressure and heat flux. The opposing jet interacts with the freestream flow, resulting in complex physical phenomena occurring near the bow shock, the contact surface between the freestream flow and the jet, the Mach disc, the recirculation region, and the recompressed shock wave. The pressure distribution on the surface verified that the decrease in drag and heat load was directly linked to the recirculation zone and the point of reattachment on the surface.

Previous studies has extensively examined the complex flow pattern that arises from the interaction between the opposing jet and the freestream flow. The hemisphere model has been employed to investigate the impact of varying total pressure ratio on the flow characteristics and the reduction of drag in supersonic flows. According to Finley and Shang, the flow mode (SPM/LPM) of counter flow jets exhibits specific properties that vary based on the injection pressure. This phenomenon arises

due to the injection pressure, which dictates the characteristics of the expansion process at the exit of the hemisphere nozzle. When the jet from the nozzle enters the bow shock at a low injection pressure, it slightly overexpansion, causing the shock wave to be pushed away in a diamond-shaped pattern. The shock standoff distance is considerably largerthan in flows when the shock wave penetrates deeply compared to flows where there is no significant shock penetration. The flows exhibit unsteady oscillatory movements that are distinguished by the well-known diamond-shaped jet plume, commonly known as LPM. Shang [15] proposed a feedback mechanism in which the oscillatory movement is maintained by the transfer of selectively amplified frequencies from the free shear layer to the Mach disc through the embedded subsonic region. On the other hand, when the injection pressure rises, there is a certain moment at which the flow field structure abruptly transitions from LPM to SPM. When the injection pressures are high, the jet fails to penetrate the bow shock and instead forms a stable flow structure, which is referred to as the SPM. The SPM is characterized by a strong bow shock, a Mach disc, a free stagnation point, and a flow recirculation zone. The designers of supersonic and hypersonic vehicles have shown tremendous interest in the decrease of both drag and heat flux by using opposed jets that are issued from the stagnation point of a flying body. This is because opposing jets are an effective flow control technology. Hence, it is highly important, both in terms of theoretical understanding and practical implementation, to investigate and comprehend the operational mechanism of this active flow control technology.

The primary aim of this work is to conduct numerical calculations to analyze the flow properties of a counter flow jet in supersonic conditions. Numerical computations are performed to analyze the fundamental physics related to the two forms of jet interaction. Results are compared to existing experimental data, such as Schlieren pictures, and other relevant information found in literature. The study aims to analyze the impact of the total pressure ratio and the transition from the unstable LPM to the more stable SPM in order to further our comprehension of the interaction between shock waves and shear layers. This paper will further analyze the influence of the total pressure ratio on the surface pressure distribution. Specifically, it will investigate how the total pressure ratio affects the interaction between the shock wave and the shear layer, the size of the recirculation zone, and the position of the reattachment point in the SPM. Another aspect of this study is to explore the unsteady oscillatory motions in the LPM. Several researchers[20-21] have analyzed the physical principles governing these occurrences using the Proper Orthogonal Decomposition (POD) technique. Nevertheless, there are several physical phenomena that still lack understanding and are of considerable interest for further comprehensive investigations. These include the interaction between shock waves and shear layers, which leads to the unsteady movement of the shock wave, as well as the formation of unstable spatially growing hydrodynamic waves due to shear layer instabilities. To understand these unsteady flow structures evolution, this paper utilizes Dynamic Mode Decomposition (DMD) extract the dominant flow structures for the developing opposing jets, and to comprehend the progression of these structures and determine the factors that influence their growth and decay, in purpose of gaining insights into the underlying mechanisms of linearity and nonlinearity in the jet flow fields. Through DMD, the clear identification of dominant structures with the relevant frequency, as well as the observation of growth or decay characteristics and the spatial evolution associated with each DMD mode.

In the following sections, flow configurations and a brief description of the computational methods are given in Section 2. Section 3 discusses the opposing jet in supersonic flows study of the hemispherical model mentioned earlier, followed by a brief summary in Section 4.

## 2. Methodology and Problem Description

# 2.1 Numerical method

An in-house Hybrid-Unstructured-mesh-based 3D Navier-Stokes solver (HUNS3D)[22] is adopted to simulate the flowfield numerically. HUNS3D use the finite volume method to solve the three-dimensional compressible Navier-Stokes equations in generalized coordinates. And it has been extensively described in earlier references[23-24] for its effective implementation in fundamental research on multidisciplinary coupling and complex turbulent flow simulation. The equation of state employed is that of an ideal gas, but the molecular viscosity is assumed to conform to the Sutherland law. In order to remove the dimensional aspects of the equations, we employ the free stream

variables and the diameter of the hemisphere  $d_m$ , as reference values.

Research indicates that the SST  $k-\omega$  turbulence model is more effective in accurately representing the flowfield properties of opposing jet, including shockwaves, separation, and recirculation zones. Furthermore, in order to examine a jet emanating from a blunt object against a supersonic stream, the initial and boundary conditions are given as follows. The initial condition is set as the free-stream quantities. No-slip and adiabatic conditions are applied on the body surface. The far-field boundary and downstream boundary conditions are treated by a characteristic method based on Riemann invariants. The inlet boundary condition[Blazek] is incorporated into HUNS3D. This jet boundary condition can be employed to model the characteristics of subsonic and supersonic opposing jet flows.

# 2.2 Dynamic Mode Decomposition

In this section, the method of DMD is outlined briefly. DMD is a powerful method for analysing the dynamics of nonlinear systems using data generated either computationally or experimentally. The method, first developed by Schmid[25], is based on Koopman modes and identifies the low-order dynamics describing the flow field that are actually governed by the infinite dimensional Navier–Stokes equations. The DMD modes are spatial fields representing coherent structures in the flow associated with a distinct oscillatory frequency.

Schmid has provided a clear explanation of the dynamic mode decomposition algorithm[25]. This study involves conducting DMD analysis on a time series dataset. Consider a sequence of data vectors  $V_1^N = \{v_1, v_2, \cdots, v_N\}$ , where N is the number of snapshots forming the sequence of data and each  $v_i$  represents the ith flow fields. Assuming the flow field  $v_{i+1}$  can be represented by the flow field  $v_i$  by a linear mapping A

$$v_{i+1} = Av_i \tag{1}$$

Using (1), the sequence in  $V_1^N = \{v_1, v_2, \dots, v_N\}$  can be reformulated as

$$V_1^N = \{v_1, Av_1, \dots, A^{N-1}v_1\}$$
 (2)

For a sufficient large number of N, Assuming the last vector  $v_N$  can be expressed by a linear combination of previous vectors[26]

$$V_2^N = AV_1^{N-1} = V_1^{N-1}S + re_{N-1}^T$$
(3)

Where the companion matrix S can be easily solved using a QR-decomposition of  $V_1^{N-1}$ . The matrix S gives eigenvalues  $\lambda$  and eigenvectors  $\omega$ . Using the ith eigenvector  $\omega_i$ , it is easy to get the ith the scaled DMD modes  $\phi_i$  whose amplitude  $\|\phi_i\|$  is defined as

$$\|\phi_i\| = \sqrt{\operatorname{Re}(\phi_i)^2 + \operatorname{Im}(\phi_i)^2} \tag{4}$$

Where  $\|\phi_i\|$  can be used to sort the mode.

### 2.3 Problem Description

We consider a supersonic flow with a free-stream Mach number  $Ma_{\infty}=2.5$  around a hemispherical nose perturbed by an opposing sonic jet placed on its axis. As shown in Figure 1, the configuration of the model is a hemispherical blunt body with a diameter  $d_m$ . The diameter of the sonic nozzle is  $d_j$ . And the flow field influenced by opposing jets appears as shown in Figure 2. Based on previous experiments [6], an ideal gas is assumed for the free stream and the jet. The total pressure, the total temperature, and the Mach number of the free-stream at infinity are expressed by  $P_{0,\infty}$ ,  $T_{0,\infty}$ ,  $Ma_{\infty}$ , respectively, and those for the opposing jet are represented by  $P_{0,j}$ ,  $T_{0,j}$ ,  $Ma_j$ , respectively. Figure 1(b) shows the computational grid distribution in this research. The numerical analysis model was intentionally built to be identical to Finley[6] for the purpose of comparison.

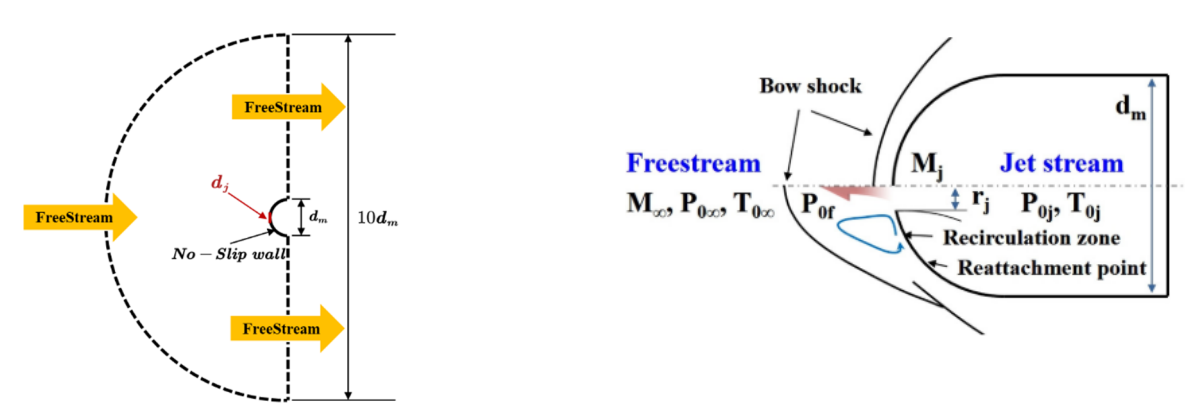


Figure 1 – Source area for computation domain.

Figure 2 – Principal features of opposing jets.[17]

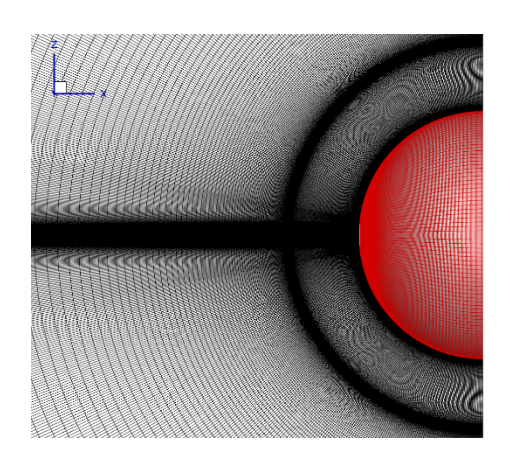


Figure 3 – Numerical grid distribution details.

The freestream gas and opposing jets are air, and the flow conditions of the freestream and the opposing jets are shown in Table 1.

	Parameter	Value	
Freestream	Mach number	2.5	
	Stagnation pressure[kPa]	275	
	Stagnation temperature[K]	294	
Opposing jets	Mach number	1.0	
	Stagnation pressure[kPa]	148~231	
	Stagnation temperature[K]	294	
	$R(d_m/d_j)$	7.6	
	Wall temperature[K]	294	

Table 1 Conditions of freestream and opposing jets.

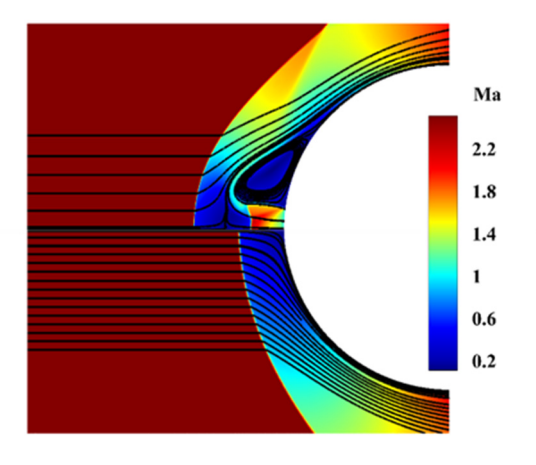
#### 3. Results and Discussion

In this section, to investigate the effect of jet pressure on flow field, several groups of flow cases with different total pressure ratio  $Pr=\frac{P_{0j}}{P_{0f}}$ , where  $P_{0f}$  is the pitot pressure of the free-stream, are studied.

#### 3.1 Validation tests

A validation test for the same flow but with an opposing jet is carried out, both the results with and without the jet are presented in Figure 2 together with the experimental data. Figure 2(a) shows the Mach number contour near around the front area of the body with no jet where a bow shock standing in front of the body is clearly simulated. In the scenario where there is a opposing jet at Pr = 1.68, the distribution of the Mach number for the case with the jet is apparently different from the case without jet, as shown in Figure 2(a). Figure 2(b) shows the mixing flow structure where the experimental schlieren image of Finley's[6] is also placed in the figure for comparison. Obviously,

the flow characteristics of the numerical schlieren-like visualizations are consistent with the experimental schlieren image. And it is observed from Figure 2(b) that iso-contours of  $\|\nabla \vec{\rho}\|$  in the meridian planes for Pr=1.68 exhibits two distinct shock waves (labeled bow shock and terminal shock), which is said to be SPM. Within the context of the SPM, the presence of a jet flow causes the bow shock in front of the body to be displaced further away from the body surface, resulting in a noticeably increased bow shock stand-off distance compared to when there is no jet flow. Evidence clearly demonstrates the formation of a protrusion boundary interface between the jet flow and the free-stream. Additionally, it is observed that the fluid emitted from the jet changes its direction, forming a conical layer of freely flowing fluid. This layer partially mixes with the surrounding fluid, creating a region of recirculation. The size of this recirculation region and the point at which the fluid reattaches are influenced by the Pr. Figure 2(b) displays the presence of Mach reflection at the jet exit, together with a distinct and well-defined Mach disc.





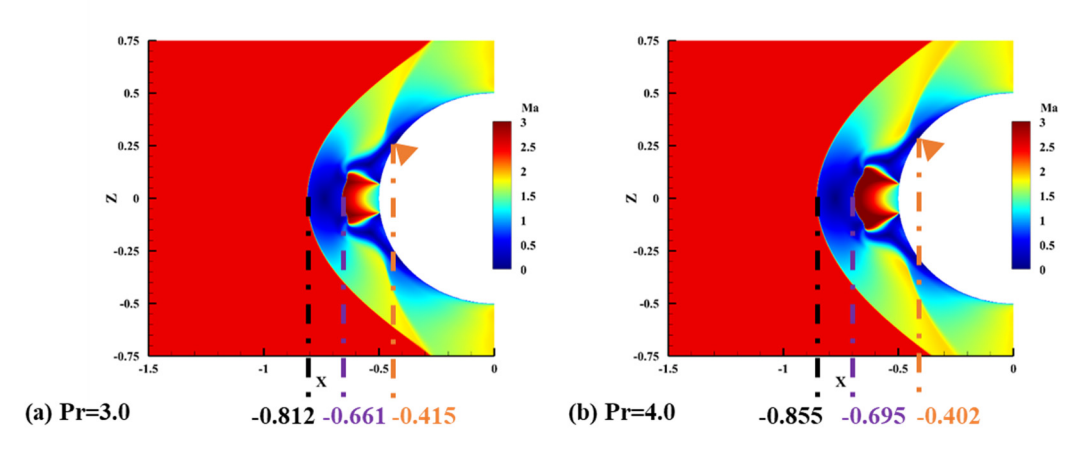
- (a) Mach number contour and streamline with no jet and jet (Y=0.0)
- (b) Comparison of Schlieren images at Pr = 1.68

Figure 2 – Validation test results.

In addition, we have observed two distinct flow modes that may be easily differentiated based on the overall pressure ratio, as mentioned earlier. We will conduct a more in-depth analysis of how the total pressure ratio impacts the structure of the opposing jet flow in SPM and the unsteady oscillatory process in LPM.

#### 3.2 Short Penetration Mode (Pr = 3.0 - 6.0)

In the previous study, SPM occurs at higher Pr. It is found that both the shock stand-off distance and the shockwave structure settle to a nearly steady state. The shock stand-off distance keeps nearly a constant and there is no periodically change in the flow structure and the stand-off distance. To examine the attributes of the total pressure ratio in SPM, we systematically varied the total pressure ratio to 3.0, 4.0, 5.0, and 6.0.



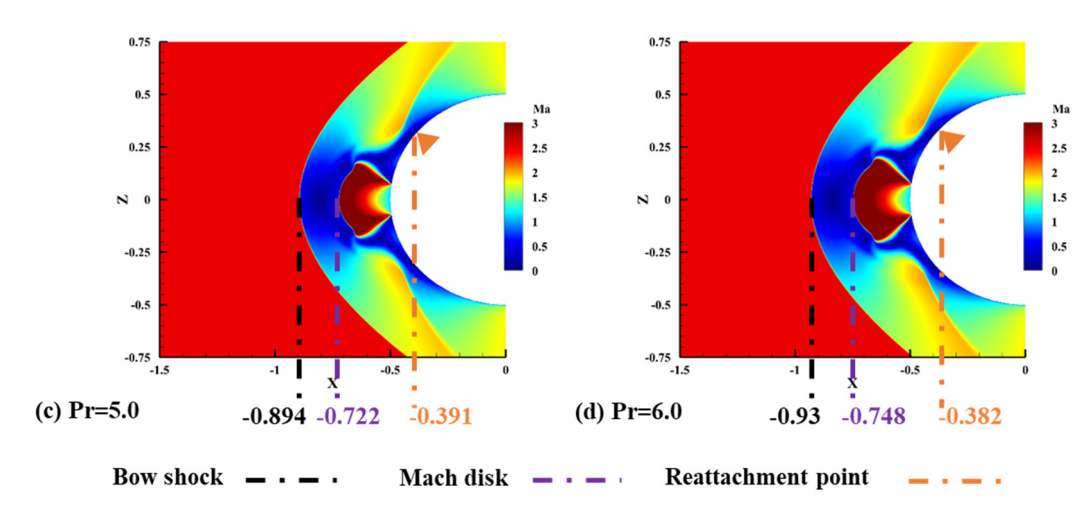


Figure 3 – Mach number contours with different total pressure ratio.

Figure 3 shows the Mach number contours with different total pressure ratio. As can be seen in Figure 3 clearly demonstrates that the size of the flow field varies noticeably, and the penetration length increases with higher total pressure ratios. Within the context of SPM, the injected flow experiences a significant expansion, causing the expanding jets to exhibit identical behavior to that observed at the same place on the Mach disc. In Figure 3(a), the position of the Mach disc is located at X=-0.661, and as the total pressure ratio increases, the greater the jet expansion, the further back the Mach disc is positioned. On the other hand, the bow shock stand-off distance gradually increases from 0.312(Pr=3.0) to 0.43(Pr=6.0) with the increase of the total pressure ratio.

Currently, we are examining the relationshipbetween the total pressure ratio and the flow characteristics of the recirculation zone, as well as the reattachment point. The literature[17] states that the recirculation zone mechanism is the balance between the mass flow entering the recirculation zone at the reattachment point and the mass flow exiting the recirculation zone. Due to the higher pressure at the reattachment point, a flow is formed that enters the recirculation zone. The interface located at the outside boundary of this recirculation zone consistently exhibits a total pressure that surpasses that of the reattachment point. The flow, characterized by a relatively high total pressure, surpasses the static pressure at the reattachment point and continues to move in the downstream direction. Figure 3 demonstrates that as the total pressure ratio increases, the interface at the outer boundary of the recirculation zone has a higher total pressure compared to the reattachment point. Additionally, the reattachment point tends to be located further away from the central line. Consequently, this causes the size of the recirculation zone to increase. The distance of the reattachment point from the central line directly correlates with the expansion of the low-pressure region in the recirculation zone. Consequently, numerous prior studies [17-19] have utilized the low pressure flow features of the recirculation zone to achieve drag reduction.

### 3.3 Long Penetration Mode (Pr < 1.52)

The LPM occurs when the injection pressure is relatively low, and highly unsteady flows in which the shock wave oscillates forward and backward are observed in the LPM, which is characterized by the presence of an X-type structure in the plane and the termination of the jet column at a Mach disc. As mentioned above, when the injection pressure exceed a critical value, the flow mode changed from LPM to SPM, and in the current study, the critical value  $P_{crit} = 1.52$ . In order to analyze the flow characteristics of LPM, this paper simulate the opposing jet at Pr = 1.25 and Pr = 1.48.

#### 3.3.1 Flow characteristics at LPM

Figure 4 displays the numerical expanded schlieren pattern for Pr= 1.48, which effectively demonstrates the flow features in the LPM. According to Figure 4, The LPM flow exhibits a series of expansion waves and the interaction region is formed as an X-shaped structure. The periodic oscillation indicated earlier in LPM can be attributed to a feedback mechanism originating from the unstable conical shear layer towards the Mach disc of this flow field.



Figure 4 – Numerical schlieren-like visualizations using contours  $\|\nabla \vec{\rho}\|$  in the meridian Plane (Pr=1.48).

Figure 5 shows the flow characteristics under different total pressure ratios at LPM. Given that the flow structure of the LPM is oscillating, Figure 5 displays the Mach number contours of the flow field at the point of maximum penetration length during one oscillation period. Obviously, the penetration length at Pr = 1.48 is longer than Pr = 1.25. At low injection pressure, the penetration length is reduced due to the lesser mass or momentum flux of the injection flow compared to the inflow condition.

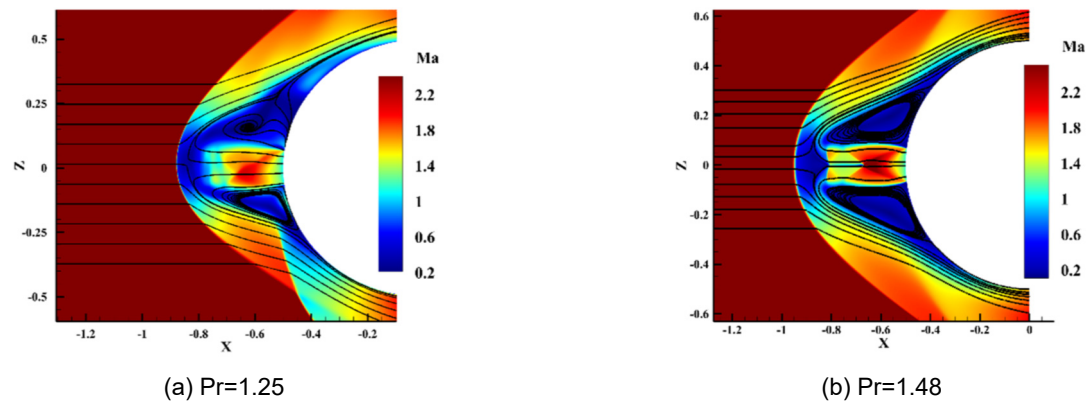


Figure 5 – Mach number contours and streamline with different total pressure ratio at LPM.

# 3.3.2 Analysis of oscillation characteristics

A group of instantaneous pressure contours at four different moments of one oscillation cycle T is shown in Figure 7(a) to (d), where the flow structures and the stand-off distance of the shock change periodically, which eventually result in the time histories of drag coefficient on the body surface periodical oscillation shown in Figure 6.

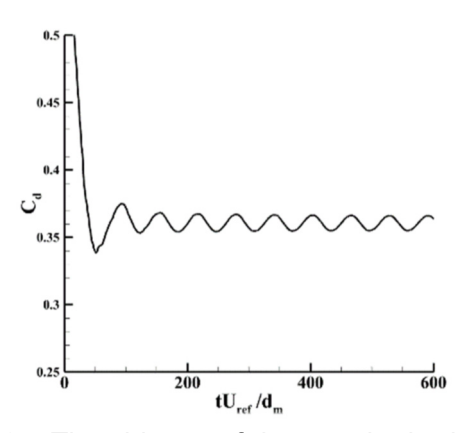


Figure 6 – Time history of drag on the body surface.

In addition, the shock wave oscillation is extremely unsteady and presents a distorted shape. The shape and oscillation of the bow shock are relatively asymmetric. This is consistent with the previous research conducted by Kim[27] in their experimental and numerical analyses. In this situation, the jet flow is unable to stay contained within the shock layer. On the other hand, it leads to a significant interaction with the bow shock,, which creating an unstable flow pattern. But compared with Pr=1.25, The shock wave remains asymmetric and distorted but more mitigated than Pr=1.48 from Figure 4. From Figure 7, The periodic oscillation of the shock wave leads to the periodic change of the recirculation region and the corresponding reattachment point, leading to the model surface experiencing periodic oscillations in pressure. As previously stated, the decrease in surface pressure at the recirculation zone is anticipated to have a positive impact on drag reduction. Nevertheless, the findings indicate that it is crucial to pay close attention to the reattachment point, where there is a substantial increase in pressure and periodic oscillation, during the occurrence of LPM.

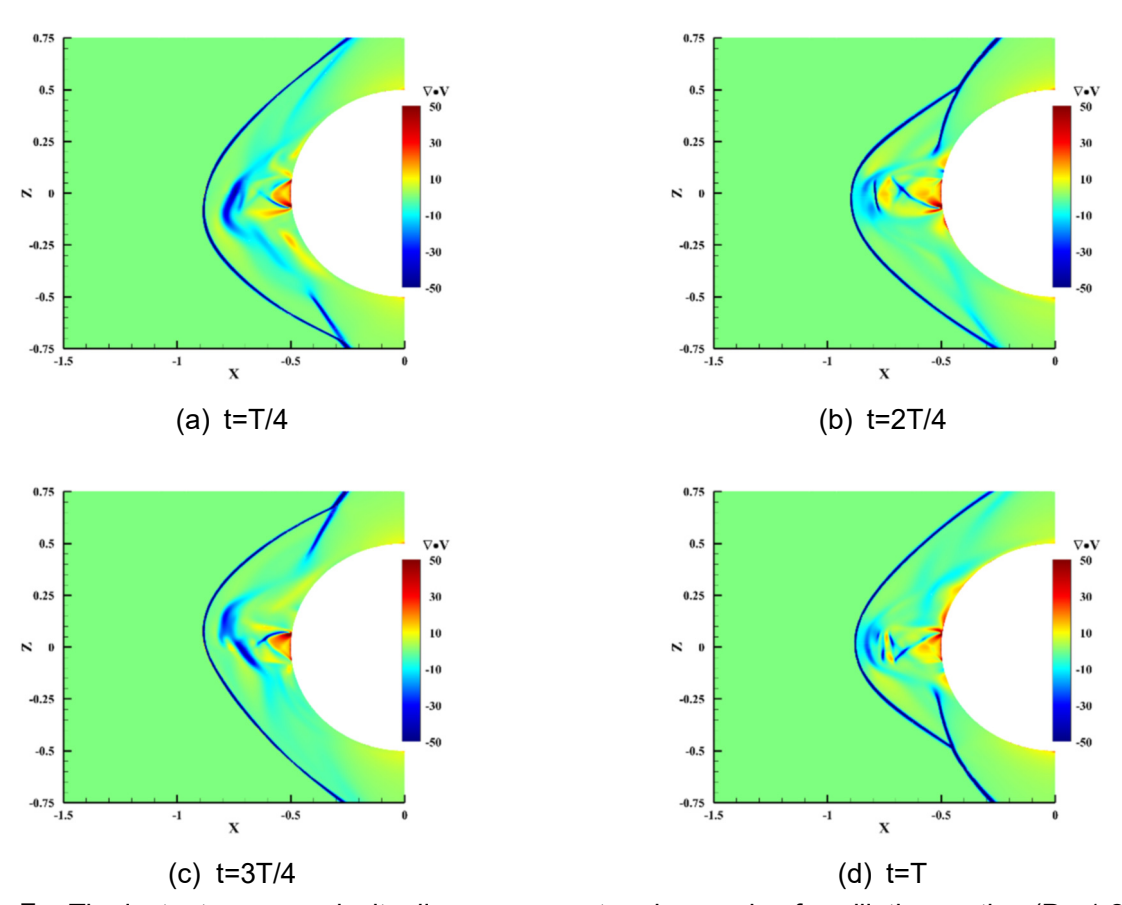
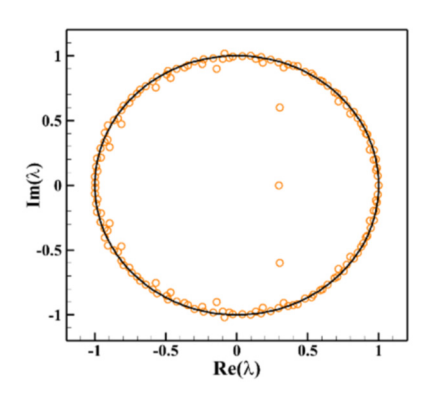


Figure 7 – The instantaneous velocity divergence contour in a cycle of oscillation motion (Pr=1.25). As stated above, this work utilizes the DMD approach to quantitatively examine the LPM flow by extracting the global oscillatory behavior from the numerical data. A total of 1000 equally spaced snapshots in time are employed to execute the DMD at Pr=1.25. The analysis has been conducted using the streamwise velocity component, which is dominant among the three components. Figure 8(a) shows the dynamics of DMD, as most of DMD modes lay nearby the unit circle. Figure 8(b) illustrates the distribution of energy attributed to pressure variations in each DMD mode, as well as the total accumulated energy. In Figure 8(b), it can be observed that for the Pr=1.25, the first three modes account for approximately 58% of the total energy.



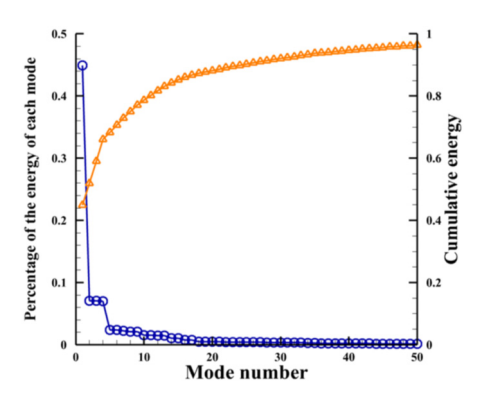


Figure 8 – (a) eigenvalues of DMD modes (left)

(b) Percentage of the energy of each mode and cumulative energy in the jet (right).

Figure 9 displays the spatial shape of the first three modes in the cross-section plane at x/D = -0.75 for various total pressure ratios. The DMD mode 1 depicts the average velocity distribution, demonstrating the opposing flow of the jet as it reaches the freestream. The spatial distributions of the first three DMD modes at Pr=1.25 exhibit clear antisymmetric patterns, whereas the axisymmetric shapes observed in the first three DMD modes at Pr=1.48. This discovery aligns with the off-axis flow movement observed in the cross-sectional plane illustrated in Figure 7. Therefore, the examination of the flow patterns in the unstable states can be attributed to the self-sustained movements mechanisms described by Chen[21]. Due to the prevailing movement of the conical shear layer with a Pr=1.25, it displays an antisymmetric nature. Chen[21] effectively applies the concept[28] of the feedback model to the unstable condition.

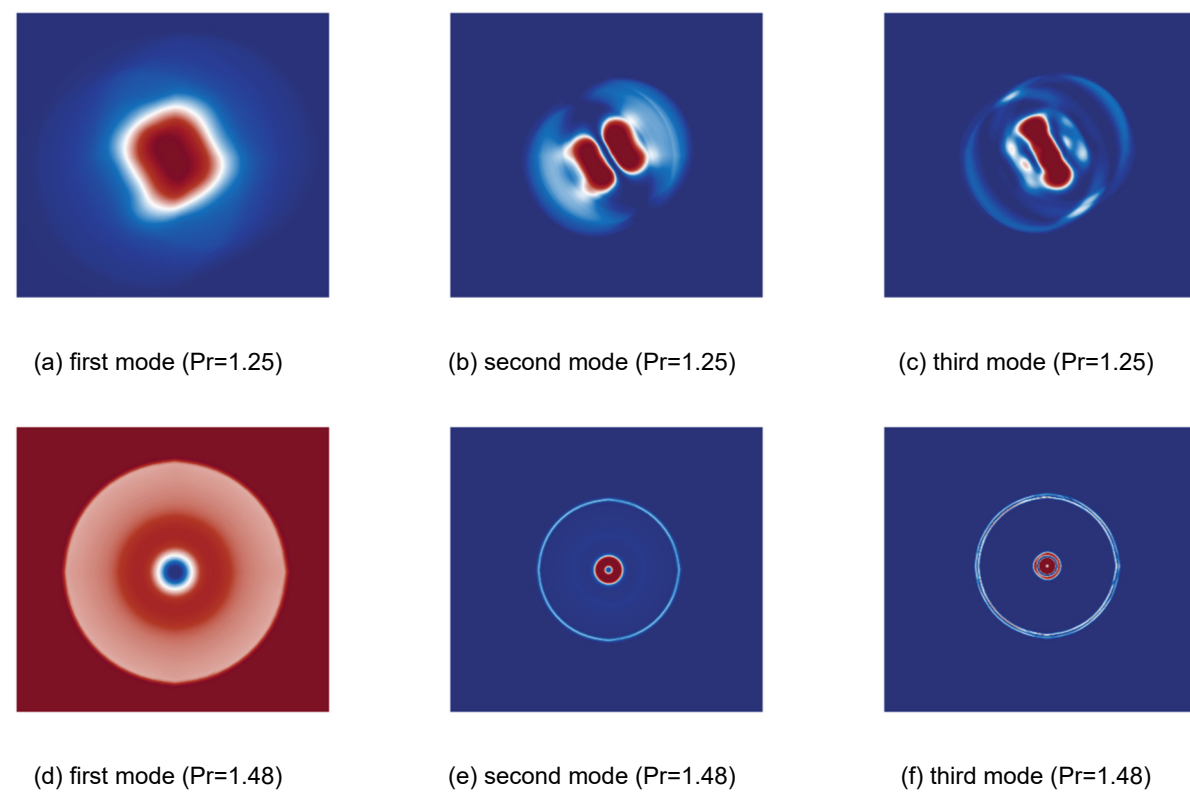


Figure 9 – Spatial distributions of the first three DMD modes at Pr=1.25 and Pr=1.48.

Figure 10 depicts three instances in the temporal progression of the DMD second-order mode during its evolutionary history. By observing the image, it is evident that the streamwise velocity direction of the DMD second-order mode exhibits periodic alternations between positive and negative values over time. This suggests that the primary mode of the DMD second-order mode governs the flow and induces asymmetric motion. Upon examining the development of DMD second-order modes, it is noted that the conical shear layer exhibits an off-axis flapping motion. In addition, waves that

propagate downstream occur alternately on both sides.



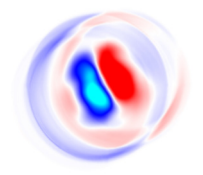




Figure 10 – Spatial distributions of the second DMD modes at different times.

Figure 11 depicts the mode shape distributions of the first three modes in the cross-section plane at y=0.0. The dominant modes display the characteristic of symmetric motion,, which is linked to the corresponding spatial structures in the y=0.0 plane as well as interactions between different regions of the flow domain. Figure 11(a) shows that the DMD modes 1 is the mean velocity field, which means the opposing jet entering the freestream flow. DMD modes 2 represent the shear layer generated between the freestream and the opposing jet. Upon observing the temporal evolution of modes 2, it becomes evident that the shear layer region exhibits periodic fluctuations in velocity, alternating between positive and negative values. This behavior indicates that this mode also captures the oscillatory vertical motion of the flow. However, the persistent temporal symmetry of DMD modes 3 indicates that this mode accurately captures the velocity of the flow in the direction of the flow.

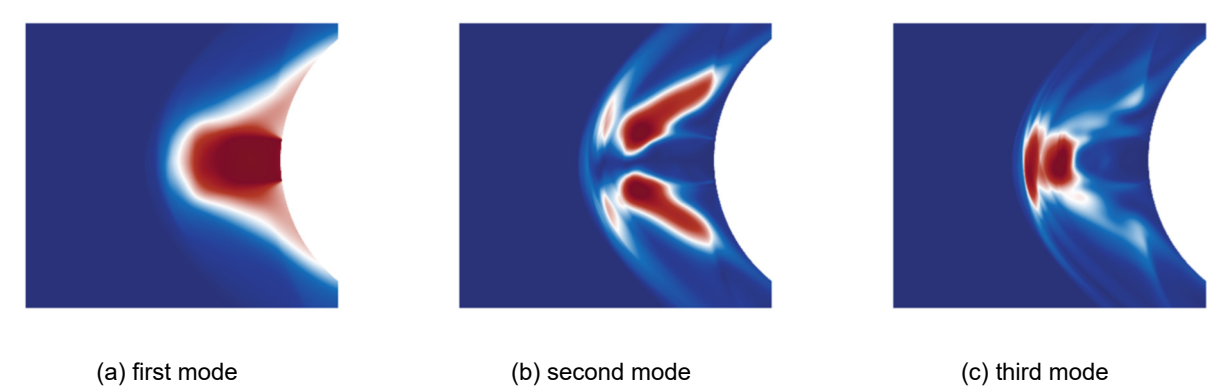


Figure 11 – Spatial distributions of the first three DMD modes at Pr=1.25 (Y=0).

## 4. Conclusion

A numerical simulation is conducted to study the flow characteristics of a sonic jet originating from a spherical body in opposition to a supersonic flow at Mach 2.5. The effects of opposing jets on the flow field are investigated using computational simulations at different total pressure ratios. Two distinct flow motion modes are identified: an oscillatory unsteady mode characterized by a multiplecell structure in the jet column, with a larger shock stand-off distance; and a nearly steady mode characterized by a single-cell structure, with a well-established Mach disc at the end of the jet column and a shorter stand-off distance. At a low injection pressure value, the flow consistently exhibits the unstable oscillatory motion mode (LPM) at  $Pr < P_{crit}$ . However, as the injection pressure was raised, the flow shifted to the virtually steady motion mode (SPM) at Pr >  $P_{crit}$ . For the SPM, increasing the injection pressure led to an increase in the penetration length and caused the reattachment point to be pushed downstream. For the LPM, the unsteady oscillatory motion is nearly axisymmetric at the larger Pr, but with the decrease of the Pr, the asymmetric motion was closely observed, characterized by a flapping motion in the recirculation zone. The computational results are used to analyze the unstable motion in the LPM using the DMD technique.. It was noted that DMD analysis has proven to be an effective tool of analyzing dynamic features, correctly capturing flow characteristics in the LPM. Furthermore, this research suggests that the spatial distributions of DMD modes exhibit axisymmetric patterns at higher total pressure ratios, but asymmetrical patterns at lower total pressure ratios. Ultimately, the analysis of individual components utilizing DMD mode demonstrates that the DMD modes 2 is accountable for the observed unsteady motions in the flow.

# **Acknowledgements**

The research was supported by the National Natural Science Foundation of China (No.U2141254, and No.U23B6009). The computations were conducted in Computing Center in Xi'an. The authors thankfully acknowledge these institutions.

## **Copyright Statement**

The authors confirm that they, and/or their company or organization, hold copyright on all of the original material included in this paper. The authors also confirm that they have obtained permission, from the copyright holder of any third party material included in this paper, to publish it as part of their paper. The authors confirm that they give permission, or have obtained permission from the copyright holder of this paper, for the publication and distribution of this paper as part of the ICAS proceedings or as individual off-prints from the proceedings.

#### References

- [1] Shen B X, Yin L, Zhang X L, et al. Investigation on cooling effect with a combinational opposing jet and platelet transpiration concept in hypersonic flow[J]. Aerospace Science and Technology, 2019, 85: 399-408.
- [2] F. Deng, F. Xie, N. Qin, W. Huang, L. Wang, H. Chu, Drag reduction investigation for hypersonic lifting-body vehicles with aerospike and long penetration mode counterflowing jet[J]. Aerospace Science and Technology, 2018, 76: 361-373.
- [3] Zhu L, Li Y, Chen X, et al. Hypersonic flow characteristics and relevant structure thermal response induced by the novel combined spike-aerodome and lateral jet strategy[J]. Aerospace science and technology, 2019, 95: 105459.
- [4] Ahmed M Y M, Qin N. Forebody shock control devices for drag and aero-heating reduction: A comprehensive survey with a practical perspective[J]. Progress in Aerospace Sciences, 2020, 112: 100585.
- [5] Bibi A, Maqsood A, Sherbaz S, et al. Drag reduction of supersonic blunt bodies using opposing jet and nozzle geometric variations[J]. Aerospace Science and Technology, 2017, 69: 244-256.
- [6] Finley P J. The flow of a jet from a body opposing a supersonic free stream[J]. Journal of Fluid Mechanics, 1966, 26(2): 337-368.
- [7] Warren C H E. An experimental investigation of the effect of ejecting a coolant gas at the nose of a bluff body[J]. Journal of Fluid Mechanics, 1960, 8(3): 400-417.
- [8] Baron J R, Alzner E. An experimental investigation of a two-layer inviscid shock cap due to blunt-body nose injection[J]. Journal of Fluid Mechanics, 1963, 15(3): 442-448.
- [9] Hayashi K, Aso S. Effect of pressure ratio on aerodynamic heating reduction due to opposing jet[C]//36th AIAA Thermophysics Conference. 2003: 4041.
- [10] Hayashi K, Aso S, Tani Y. Numerical study on aerodynamic heating reduction by opposing jet[J]. 2006.
- [11] Hayashi K, Aso S, Tani Y. Experimental study on thermal protection system by opposing jet in supersonic flow[J]. Journal of Spacecraft and Rockets, 2006, 43(1): 233-235.
- [12] Hayashi K, Aso S. Effect of pressure ratio on aerodynamic heating reduction due to opposing jet[C]//36th AIAA Thermophysics Conference. 2003: 4041.
- [13]Chen L W, Xu C Y, Lu X Y. Large-eddy simulation of opposing-jet-perturbed supersonic flows past a hemispherical nose[J]. Modern Physics Letters B, 2010, 24(13): 1287-1290.
- [14]Shang J S. Plasma injection for hypersonic blunt-body drag reduction[J]. AIAA journal, 2002, 40(6): 1178-1186.
- [15]Shang J S, Hayes J, Wurtzler K, et al. Jet-spike bifurcation in high-speed flows[J]. AIAA journal, 2001, 39(6): 1159-1165.
- [16]Blazek J. Computational fluid dynamics: principles and applications[M]. Butterworth-Heinemann, 2015.
- [17]Lee J, Lee H J, Huh H. Drag reduction analysis of counterflow jets in a short penetration mode[J]. Aerospace Science and Technology, 2020, 106: 106065.

#### Numerical Investigation of the Interaction of Opposing Jets and Supersonic Free Flows

- [18]Zhou C Y, Ji W Y. A three-dimensional numerical investigation on drag reduction of a supersonic spherical body with an opposing jet[J]. Proceedings of the Institution of Mechanical Engineers, Part G: Journal of Aerospace Engineering, 2014, 228(2): 163-177.
- [19]Lee J, Lee H J, Huh H. Drag reduction analysis of counterflow jets in a short penetration mode[J]. Aerospace Science and Technology, 2020, 106: 106065.
- [20]Iqbal M O, Thomas F O. Coherent structure in a turbulent jet via a vector implementation of the proper orthogonal decomposition[J]. Journal of Fluid Mechanics, 2007, 571: 281-326.
- [21]Chen L W, Wang G L, Lu X Y. Numerical investigation of a jet from a blunt body opposing a supersonic flow[J]. Journal of Fluid Mechanics, 2011, 684: 85-110.
- [22]Wang G, Ye Z Y. Mixed element type unstructured grid generation and its application to viscous flow simulation[C]//24th International congress of aeronautical sciences. 2004.
- [23]Li Q, Chen X, Wang G, et al. A dynamic version of the improved delayed detached-eddy simulation based on the differential Reynolds-stress model[J]. Physics of Fluids, 2022, 34(11).
- [24]Zhou H, Wang G, Mian H H, et al. Fluid-structure coupled analysis of tandem 2D elastic panels[J]. Aerospace Science and Technology, 2021, 111: 106521.
- [25]Schmid P J. Dynamic mode decomposition of numerical and experimental data[J]. Journal of fluid mechanics, 2010, 656: 5-28.
- [26]Wan Z H, Zhou L, Wang B F, et al. Dynamic mode decomposition of forced spatially developed transitional jets[J]. European Journal of Mechanics-B/Fluids, 2015, 51: 16-26.
- [27]Kim D M, Kim Y, Roh T S, et al. Observation of unsteady motion induced by counterflow jet on blunt body in hypersonic flow[J]. Journal of Visualization, 2022, 25(1): 1-14.
- [28]TAM, C. K. W. 1974 Discrete tones of isolated airfoils. J. Acoust. Soc. Am. 55, 1173-1177.